

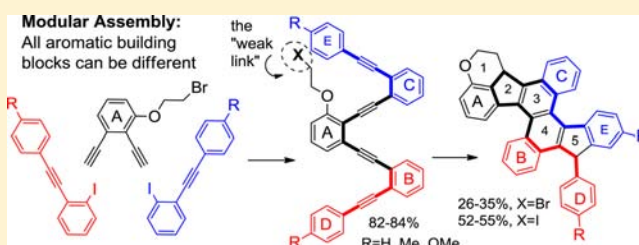
Polyaromatic Ribbons from Oligo-Alkynes via Selective Radical Cascade: Stitching Aromatic Rings with Polyacetylene Bridges

Philip M. Byers and Igor V. Alabugin*

Department of Chemistry and Biochemistry, Florida State University, Tallahassee, Florida 32306-4390, United States

S Supporting Information

ABSTRACT: Selective radical generation in conjugated oligomeric *o*-aryleneethynyls initiates an intramolecular cascade which involves *five* fast radical cyclizations followed by aromatization via a 1,5-H shift with a >93% yield per step. This radical cascade transformation opens a new avenue for the systematic and controlled preparation of functionalized graphene nanoribbons where, potentially, each of the peripheral aromatic rings can be different.

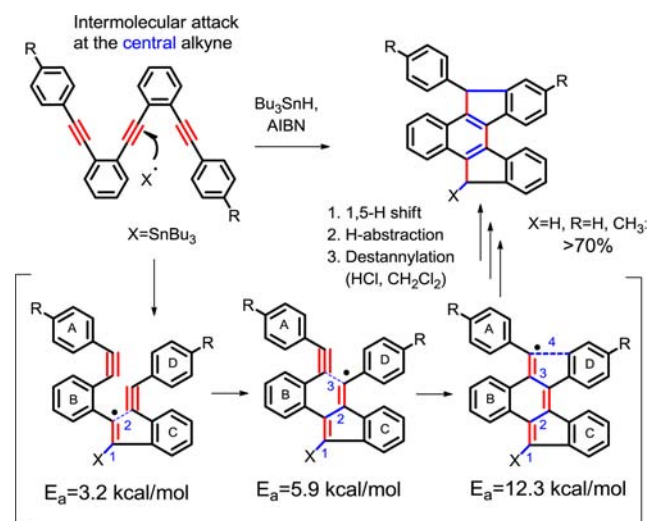


1. INTRODUCTION

Interest in polycyclic aromatic hydrocarbons (PAHs) was refueled by their structural relation to graphene, a form of carbon whose mechanical and electronic properties^{1,2} are distinctly different from those other carbon nanostructures.³ Because structural variations (e.g., size, shape, curvature,⁴ edge geometry,⁵ and composition⁶) affect electronic properties strongly, progress in this field depends on the development of rationally designed "bottom-up"⁷ approaches toward chemically and structurally uniform graphene substructures. While a number of elegant approaches⁸ to the design of symmetric graphene nanoribbons have been reported, efficient and flexible approaches to nonsymmetrically substituted graphene nanoribbon structures are scarce.⁹⁻¹¹ These approaches become even more valuable considering recent reports where relatively large polycyclic aromatic hydrocarbons were used to create even larger carbon nanostructures using surface-assisted coupling¹² and template-initiated growth.¹³

Alkyne functionality is an attractive entry point for the preparation of carbon-rich materials¹⁴ due to its high carbon content (atom economy), the possibility of modular assembly via reliable cross-coupling chemistry, and the propensity of alkynes to participate in well-choreographed cascade transformations leading to the rapid construction of polycyclic frameworks.¹⁵ These advantages are illustrated by the recently reported radical cascade transforming triynes (1,2-bis(2-arylethynyl)phenyl ethynes) into an extended polyaromatic system (benzo[*a*]indeno[2,1-*c*]fluorene) in >70%.¹⁶ The efficiency of this cascade hinges on the chemoselective *intermolecular* attack of tributyl tin (Bu_3Sn) radical at the *central* alkyne of the triyne system (Scheme 1). This step initiates an efficient cascade, where each of the subsequent steps (5-exo-dig, 6-exo-dig cyclizations, attack at the aromatic ring, and 1,5-shift-induced rearomatization) has a low barrier following a favorable energy landscape to progressively more and more stable intermediates.

Scheme 1. B3LYP Calculated Barriers for Radical Cascade Transformation of Tris-*o*-aryleneethynyls via Selective Intermolecular Activation



Mechanistic studies, together with DFT computational analysis, revealed the reasons for this efficiency and suggested that this cascade can be expanded to the preparation of larger molecules of different sizes and architectures. In particular, we were encouraged by the lower calculated barriers for the key 5-exo-dig and 6-exo-dig cyclization steps¹⁷ (~ 3 and ~ 6 kcal/mol, respectively) relative to the barrier for the final ring formation via radical attack at an aromatic system (12 kcal/mol, Scheme 1). According to these values, the final cyclization step is ~ 100 000 times slower than the 6-exo-dig closure on the pendant alkyne. The energetics suggest that if the starting material had

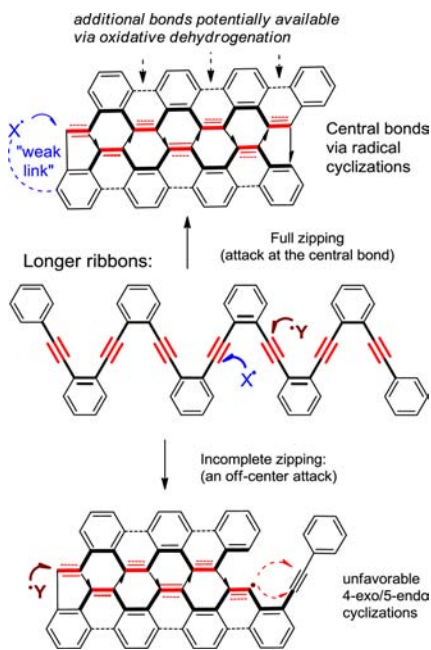
Received: September 9, 2011

Published: May 23, 2012

additional triple bonds capable of extending the cascade, preparation of larger carbon nanostructures would be feasible.

However, when we applied intermolecular initiation to the longer polyynes, the selectivity decreased dramatically and complex mixtures were formed.¹⁸ For this cascade to go to completion, the radical cascade must be initiated via selective attack at the *central* alkyne. Attack at any other alkyne would require an unfavorable cascade that involves a relatively inefficient¹⁹ 5-endo (or 4-exo) closure (Scheme 2).

Scheme 2. Proposed Extension of the Alkyne Radical Cascade towards Longer Graphene Ribbons and Importance of Selective Radical Attack at the Central Alkyne



2. RESULTS AND DISCUSSION

2.1. Enediyne Synthesis and Radical Cascades.

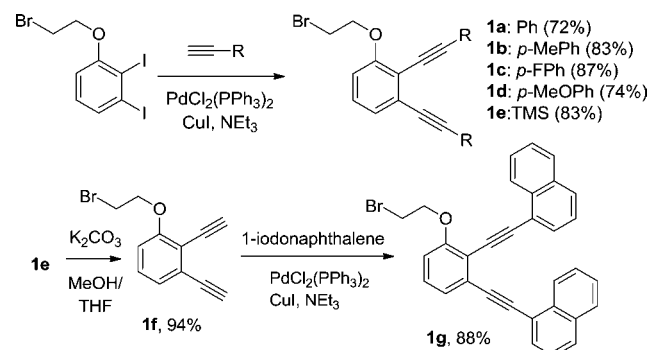
The similarity of electronic and steric properties of alkynes in the larger polyalkyne oligomers precludes selective intermolecular radical attack at the central alkyne. We describe here a strategy that targets the central alkyne by intramolecular radical attack. A suitable initiator (the “weak link”) is built-in directly at the central ring to ensure that the cascade begins at the right part of the molecule. Selective radical formation in the presence of multiple triple bonds initiates the complete “zipping” of the oligo alkynes into a fully aromatic ribbon.

Since radical cascades are often compatible with a variety of functional groups,¹⁵ we have concentrated on radical initiation of the cascade. Because finding suitable conditions for the chemoselective alkyl radical generation in the presence of multiple alkynes is challenging, we turned to model compounds with two triple bonds (enediynes).

We chose the first intramolecular step in the radical cascade to 6-exo-dig closures to avoid the unfavorable arrangement of two fused five-membered rings.^{17c} The requisite library of enediynes was synthesized through the Sonogashira reaction of 1-(2-bromoethoxy)-2,3-diiodobenzene with a number of substituted alkynes **1a–1e**. Bis-1-naphthyl enediyne **1g** was prepared through a slightly different procedure based on

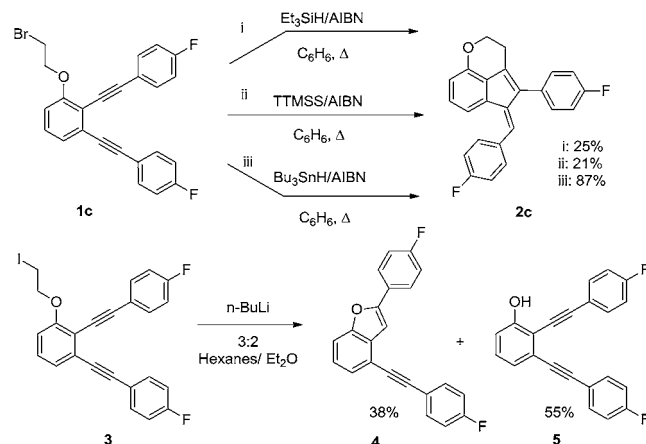
Sonogashira coupling of the terminal enediyne **1f** with 1-iodonaphthalene (Scheme 3).

Scheme 3. Synthesis of Enediyne Compounds for Model Radical Cascade Reactions



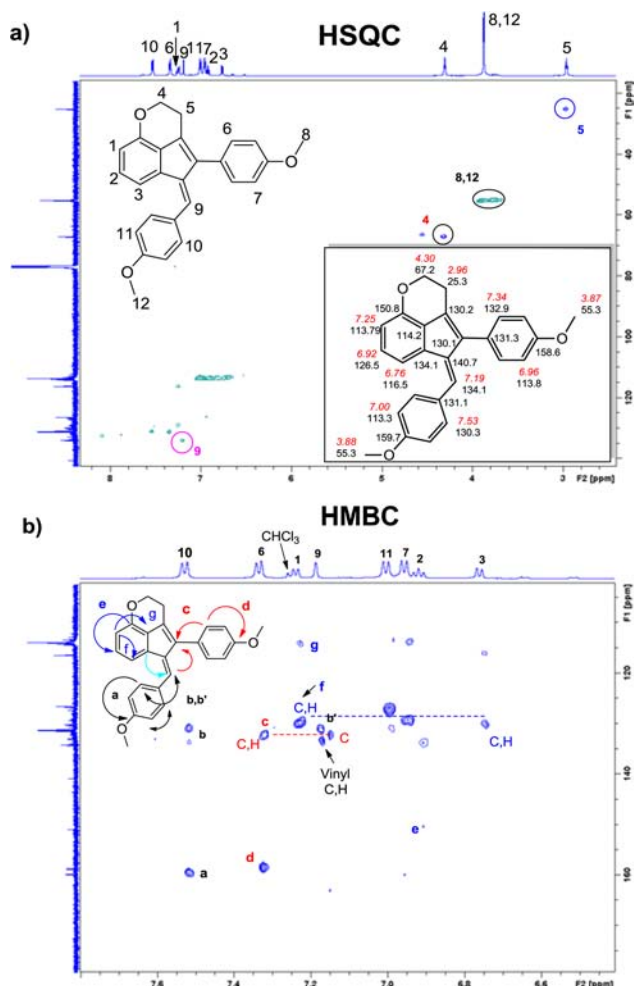
Our initial efforts using triethylsilane and tris(trimethylsilyl)silane (Et_3SiH and TTMSS) led to the products of the desired cascade transformation. However, the reactions were sluggish and the yields were low (21–25%). A dramatic increase in efficiency was observed when the $\text{Bu}_3\text{SnH}/\text{AIBN}$ system was used for the chemoselective cascade initiation. We also attempted anionic 6-exo-dig cyclization but found that phenoxide elimination dominates, leading to compounds **5**, which can be converted into heterocycle **4**, via an anionic 5-endo-dig closure (Scheme 4).

Scheme 4. Optimization of Cascade Conditions



Selective radical attack at the alkyl halide in the presence of two alkynes is remarkable considering that alkynes are also reactive under these conditions.²⁰ Structures of the cascade cyclization products were elucidated by heteronuclear single quantum coherence (HSQC), heteronuclear multiple bond correlation (HMBC) and nuclear Overhauser effect (NOE) NMR experiments. The 2D experiments confirmed that products originate from the 6-exo-dig, 5-exo-dig cascade. Results for the cyclization of the *p*-methoxy substituted enediyne are discussed in more detail.

No gHMBC correlations for the vinyl C–H and the C3–H at the trisubstituted benzene ring were observed (Scheme 5). The lack of correlation implies that a 5-exo-dig cyclization took place in the second step giving an exocyclic double bond. The product of an endo-dig cyclization would be expected to display

Scheme 5. HSQC and HMBC Experiments for the Cyclization of *p*-OMe-Substituted Eneidyne **2d**^a

^aTop HSQC NMR highlights select direct C–H couplings. The inset shows all H and C chemical shifts for enediyne **2d**. Bottom HMBC NMR shows selected C/H through-bond correlations (colored arrows).

this gHMBC correlation. All protons of the OMe-substituted rings were identified by their multiplicity and long-range couplings between the two deshielded C(–OMe) carbons and the respective aromatic meta C–H bonds (H at 7.53 couples to the carbon at 159.7 ppm and H at 7.34 ppm couples to the carbon at 158.6 ppm). One of the two meta C–H groups (7.53, 130.3 ppm) also displays a HMBC correlation with the vinyl C–H (7.19, 134.1 ppm), which identifies the terminal anisole moiety. The gCOSY spectrum shows hydrogen correlations in the methoxy-substituted benzene rings and also correlation between the CH₂'s of the –OCH₂CH₂– moiety.

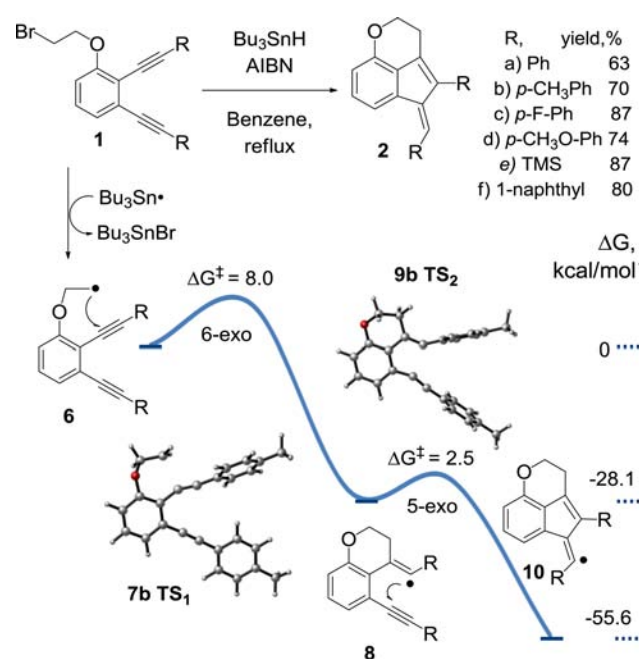
In the tricyclic core, the quaternary carbon (150.8 ppm) ipso to the oxygen of the –OCH₂CH₂– moiety shows HMBC couplings with both the aromatic meta-C–H (6.92 and 126.5 ppm) and the O–CH₂ protons (4.30 and 67.2 ppm). Both the ortho proton at 7.25 ppm and the β-CH₂ group (2.96, 25.3 ppm) correlate with the quaternary aromatic carbon (114.2 ppm) at the junction of the three cycles (see SI section for the full list of HMBC correlations), confirming that an initial cyclization followed a 6-exo-dig rather than the 7-endo-dig path. In the latter case, correlation with the β-protons would

not be expected due to the additional bond separating these atoms. Finally, protons in the CH₂ groups remain magnetically equivalent, indicating the absence of radical closure at the terminal aryl group (in contrast to the cascade transformation of tetraynes discussed in a subsequent section).

2.2. Computational Analysis of Eneidyne Cascade. As expected from general trends in alkyne cyclizations,^{16,21} both intramolecular radical attacks at the triple bonds proceed via an exoclosure leading to the selective formation of substituted 1-benzylidene-2-phenyl-3,4-dihydro-1H-5-oxa-acenaphthylenes **2**. Literature examples of two consecutive ring closures in bis-TMS-acetylenes²² are scarce. The 87% yield for the cyclization of bis-TMS-enediynes **2e** is a particularly convincing illustration for the efficiency of this radical cascade.

We have explored the cyclization potential energy surfaces for all of the enediynes computationally (Scheme 6). Several

Scheme 6. Yields and Potential Energy Surfaces for the Cascade Cyclization of Substituted Eneidyne (B3LYP/6-31+G(d,p), kcal/mol)

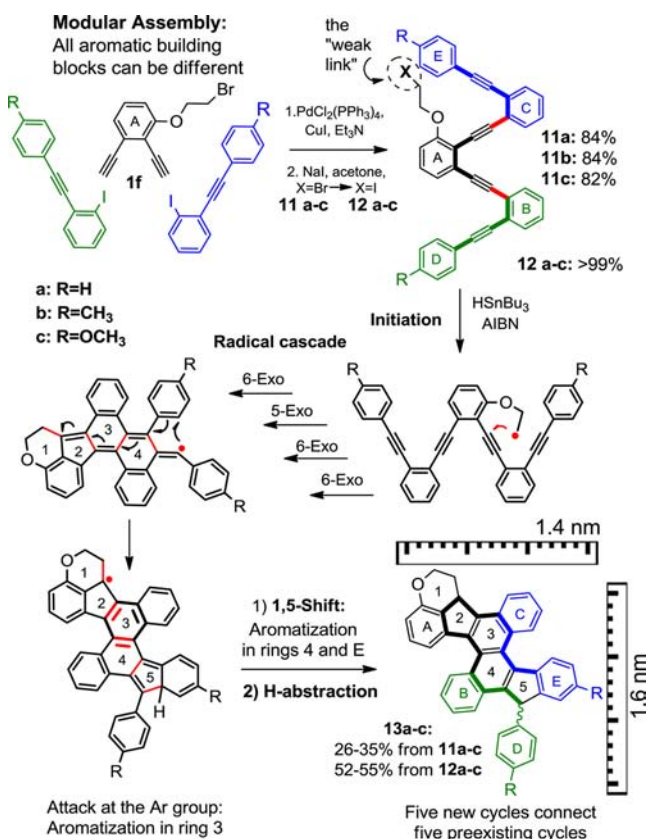


observations are noteworthy. The activation barrier for the first (6-exo) step is ~5 kcal/mol higher than the barrier for the second (5-exo) ring closure. Although both cyclization barriers are relatively insensitive to the nature of substituents in the aromatic ring (0.3–0.6 kcal/mol variations), the sterically demanding TMS group deactivates the alkyne moiety and increases the activation barriers for both cyclizations by ~2 kcal/mol. Because this additional barrier does not lead to a lower experimental yield for the cascade transformation of the TMS-substituted enediynes. (In fact, the cascade product yield is the *highest* for this substrate!) We conclude that reaction yields reflect the relative selectivity of C–Hal bond activation vs attack at a triple bond rather than relative cyclizations rates for the different substituents. Importantly, both cyclization steps are highly exothermic and irreversible and the cascade moves down the potential energy slope with each newly formed C–C bond.

2.3. Radical Cascades of Tetraynes. Encouraged by these results, we investigated the cascade cyclization of tetra-alkynes

11a–c. The fully “zipped” cascade product (Scheme 7) formed as expected. Although the yield was low for X = Br (26–35%),

Scheme 7. Synthesis of *o*-Aryleneethynylene Tetramers and the Proposed Mechanism of Cascade Transformation



the bromide can be quantitatively exchanged to form the iodo tetraalkynes **12a–c**, which transform to the fully closed nanoribbons **13a–c** in higher yields (52–55% overall,²³ ~93% per step). This increase again indicates that the reaction yields reflect the chemoselectivity of the first step (*intermolecular activation*) rather than the efficiency of the cyclizations (*intramolecular propagation*). Mass-spectrometry of side products isolated in minor amounts suggests that addition of Bu₃Sn moiety to the triple bonds is indeed still a problem.

2D HSQC and HMBC NMR analysis fully confirmed the expected polycyclic skeleton of the two diastereomers of the product (Figure 1 presents the results for this analysis for R =

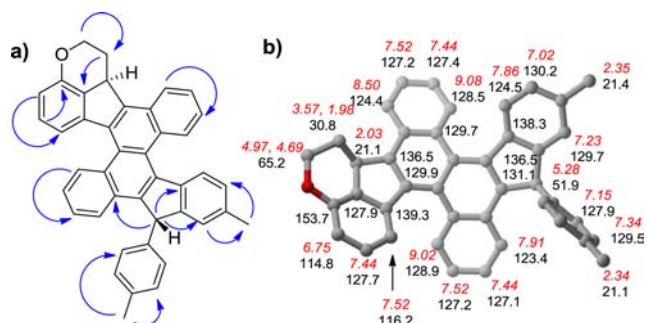


Figure 1. (a) HMBC NMR correlations used to establish the structure of cascade product **13a** and (b) H and C chemical shifts for cascade product **13a**.

Me, see SI for the details). The absence of triple bond carbon resonances confirms that cascade proceeded fully utilizing all alkynes in the process. The presence of diastereotopic CH₂ groups confirms the formation of a chirality center in the molecule. Connectivity in the OCH₂CH₂CH-moiety is supported by the 2D correlations in the gHSQC spectrum, in which the two hydrogens at 4.97 and 4.69 ppm are bound to the 65.2 ppm carbon, the two hydrogens at 3.57 and 1.98 ppm to the 30.8 ppm carbon, and the methine proton at 2.03 ppm to the 21.1 ppm carbon. For the bottom part of the ribbon, 2D correlations readily identify all carbons in the free-standing and the fused tolyl groups. The CH singlet at 5.28 ppm on the bottom part of the ribbon displays gHMBC correlations with carbons 135.8 in the ipso position of the free tolyl and 129.7 ppm carbon of the isolated CH on the fused tolyl ring. The 5.28 ppm singlet also confirms that the final cyclization and subsequent aromatization took place. Full cascade is also consistent with the presence of only one set of characteristic doublets of a *para* substituted aromatic rings. Interior aromatic carbons can be identified by comparing gHMBC with gHSQC. The presence of gHMBC cross-peaks which are not present in the gHSQC spectrum, indicates the interior quaternary carbons in the aromatic region. The ortho aromatic C–H in the central ribbon can be identified due to their significant deshielding (9.08, 128.5 and 8.50, 124.4 on the side with the fused tolyl ring and 9.02, 128.9 and 7.91, 123.4 on the other side). By identifying these outlying CH bonds along the perimeter of the structure, one can map the connections of the interior carbons (Figure 1).

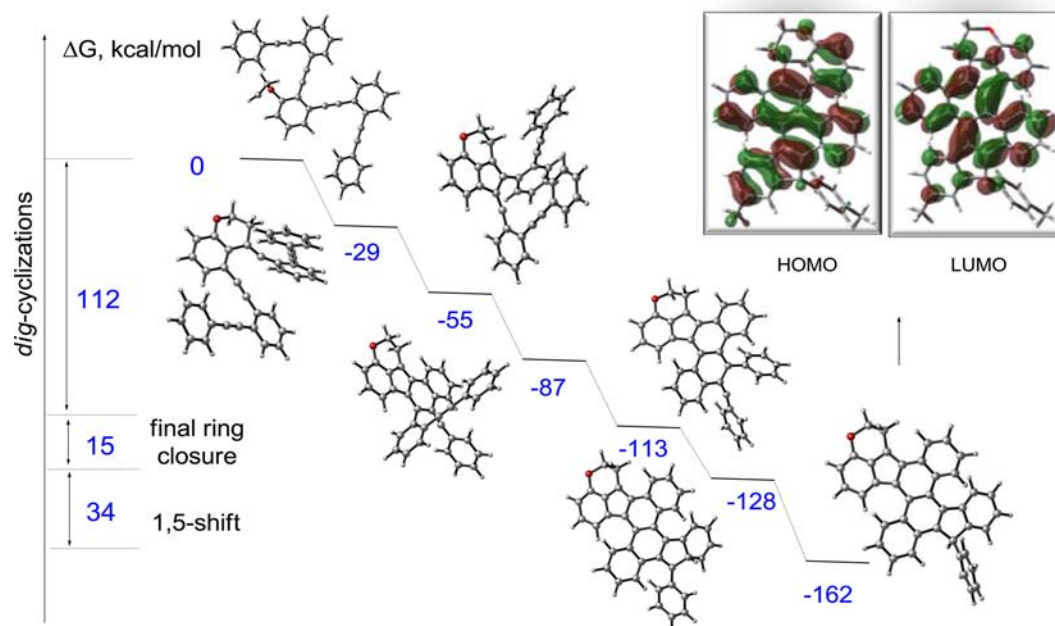
The proposed cascade mechanism is presented in (Scheme 7). Once selective activation of the “weak link” in the presence of *four* alkynes is accomplished, a cascade of *four* sequential exo-dig alkyne cyclizations occurs. Only after all four alkynes are consumed by the radical cascade does the vinyl radical attack the terminal aryl ring. This attack disrupts aromaticity in this ring and is only observed when three or more alkynes are present in the starting material (e.g., this step does not occur in the enediyne cyclizations). We suggest that, for these longer oligomers, this loss of aromaticity is partially compensated by aromatization in one of the previously formed rings (i.e., ring 3, Scheme 7). The subsequent 1,5 H-shift is also favorable ($\Delta G \approx -34$ kcal/mol) because it is assisted by rearomatization (rings 4 and E).²⁴ With each following step, this molecular system continues thermodynamic descent, resulting in an overall transformation that is ~160 kcal/mol exergonic (Scheme 8)!

The final H-abstraction step has low stereoselectivity due to the near planarity of the sterically unencumbered radical center. The fully “zipped” ribbon has good solubility in common organic solvents due to the presence of nonplanar parts in the structure. In particular, the polycyclic core is distorted due to the steric C–H interactions between *o*-hydrogens in the peripheral aryl groups.

3. CONCLUSIONS

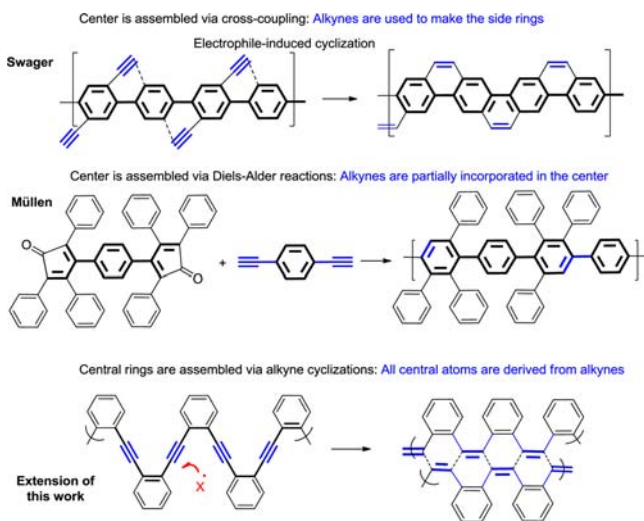
To a large extent, the highly favorable thermodynamics of the reaction cascade stems from the high energy content of alkyne functional group. This feature has been harnessed before for the preparation of graphene ribbons (Scheme 9).

For example, Swager and co-workers utilized electrophile-induced alkyne cyclizations to anneal additional cycles onto a polyphenylene backbone.²⁵ Among the many approaches developed by Müllen and co-workers for the preparation of polyaromatic scaffolds, the Diels–Alder polymerization of bis-

Scheme 8. Relative Energies and Structures of Intermediates for the Cascade Radical Transformation of Tetrynes (B3LYP/6-31+G(d,p), kcal/mol)^a

^aHOMO and LUMO for the final product 13b are given on top.

Scheme 9. Conceptual Approaches for the Use of Alkyne Functionality in Preparation of Graphene Ribbons



cyclopentadienones with bis-alkynes incorporates alkyne carbons in the backbone.²⁶

Expansion of radical cascades described in our work to longer oligoalkynes would potentially lead to the conceptually different approach toward the preparation of graphene ribbons. In this approach, the central “polyacetylene” backbone is fully assembled from the alkyne groups of the starting material via radical polymerization.

In summary, we have found that selective radical generation from alkyl halides is possible in conjugated oligomeric *o*-aryleneethynyls. Subsequent intramolecular transformation proceeds with a yield of >93% per step as a cascade of *five* fast radical cyclizations followed by aromatization via a 1,5-H shift. This radical cascade may open a new avenue for the preparation

of functionalized graphene nanoribbons where, potentially, each of the peripheral aromatic rings can be unique. Future work includes expansion of this radical cascade toward the preparation of longer and wider nanoribbons with a variety of functional groups, development of new “weak links” which avoid pentagons in the ribbon, and optimization of conditions for the further aromatization at the peripheral aromatic rings.

■ ASSOCIATED CONTENT

📄 Supporting Information

Full synthetic procedures, ¹H and ¹³C NMR spectra, and HRMS of all new compounds, gCOSY for all enediyne cascade products, gHMBC and gHMQC data for compound **2d** and **13**, DFT geometries and energies for all reactants, transition states, intermediates, and products for the cascade cyclizations of enediynes. This material is available free of charge via the Internet at <http://pubs.acs.org>.

■ AUTHOR INFORMATION

✉ Corresponding Author

alabugin@chem.fsu.edu

Notes

The authors declare no competing financial interest.

■ ACKNOWLEDGMENTS

Support by National Science Foundation (CHE-0848686/1152491) is gratefully acknowledged.

■ REFERENCES

- (1) (a) Geim, A. K.; Novoselov, K. S. *Nat. Mater.* **2007**, *6*, 183. (b) Castro Neto, A.; Guinea, F.; Peres, N. M. R.; Novoselov, K. S.; Geim, A. K. *Rev. Mod. Phys.* **2009**, *81*, 109. (c) Son, Y. W.; Cohen, M. L.; Louie, S. G. *Nature* **2006**, *444*, 347. (d) Lee, C.; Wei, X.; Kyser, J. W.; Hone, J. *Science* **2008**, *321*, 385. (e) Li, X.; Wang, X.; Li, Z.; Lee, S.; Dai, H. *Science* **2008**, *319*, 1229.

- (2) (a) Allen, M. J.; Tung, V. C.; Kaner, R. B. *Chem. Rev.* **2010**, *110*, 132. (b) Zhu, Y.; Murali, S.; Cai, W.; Li, X.; Suk, J. W.; Potts, J. R.; Ruoff, R. S. *Adv. Mater.* **2010**, *22*, 3906. (c) Potts, J. R.; Dreyer, D. R.; Bielawski, C. W.; Ruoff, R. S. *Polymer* **2011**, *52*, 5.
- (3) Gogotsi, Y. *Carbon Nanomaterials*; CRC Press: Boca Raton, FL, 2006. C⁶⁰: Kroto, H. W.; Heath, J. R.; O'Brien, S. C.; Curl, R. F.; Smalley, R. E. *Nature* **1985**, *318*, 162. Carbon nanotubes: Iijima, S. *Nature* **1991**, *354*, 56. Peapods: Smith, B. W.; Monthieux, M.; Luzzi, D. E. *Nature* **1998**, *396*, 323. Diamondoids: Dahl, J. E. P.; Moldovan, J. M.; Wei, Z.; Lipton, P. A.; Denisevich, P.; Liu, S.; Schreiner, P. R.; Carlson, R. M. K. *Angew. Chem., Int. Ed.* **2011**, *49*, 9881.
- (4) Steinberg, B. D.; Jackson, E. A.; Filatov, A. S.; Wakamiya, A.; Petrukhina, M. A.; Scott, L. T. *J. Am. Chem. Soc.* **2009**, *131*, 10537.
- (5) Ritter, K. A.; Lyding, J. W. *Nat. Mater.* **2009**, *8*, 235.
- (6) Wang, X.; Li, X.; Zhang, L.; Yoon, Y.; Weber, P. K.; Wang, H.; Guo, J.; Dai, H. *Science* **2009**, *324*, 768.
- (7) For some of the advantages of the alternative "top-down" approach, see: Niyogi, S.; Bekyarova, E.; Itkis, M. E.; McWilliams, J. L.; Hamon, M. A.; Haddon, R. C. *J. Am. Chem. Soc.* **2006**, *128*, 7720. Epitaxial graphene: Berger, C.; Song, Z.; Li, T.; Li, X.; Ogbazgh, A. Y.; Feng, R.; Dai, Z.; Marchenkov, A. N.; Conrad, E. H.; First, P. N.; deHeer, W. A. *J. Phys. Chem. B.* **2004**, *108*, 19912.
- (8) Selected examples: (a) Goldfinger, M. B.; Swager, T. M. *J. Am. Chem. Soc.* **1994**, *116*, 7895. (b) Yang, X.; Dou, X.; Rouhanipour, A.; Zhi, L.; Räder, H. J.; Müllen, K. *J. Am. Chem. Soc.* **2008**, *130*, 4216. (c) Whalley, A. C.; Plunkett, K. N.; Gorodetsky, A. A.; Schenck, C. L.; Chiu, C. Y.; Steigerwald, M. L.; Nuckolls, C. *Chem. Sci.* **2011**, *2*, 132. (d) Loo, Y. L.; Hiszpanski, A. M.; Kim, B.; Wei, S.; Chiu, C. Y.; Steigerwald, M. L.; Nuckolls, C. *Org. Lett.* **2010**, *12*, 4840. (e) Chen, T. A.; Liu, R. S. *Chem.—Eur. J.* **2011**, *17*, 8023. (f) King, B. T.; Kroulik, J.; Robertson, C. R.; Rempala, P.; Hilton, C. L.; Korinek, J. D.; Gortar, L. M. *J. Org. Chem.* **2007**, *72*, 2279.
- (9) (a) Wu, J.; Pisula, W.; Müllen, K. *Chem. Rev.* **2007**, *107*, 718. (b) Müllen, K.; Wegner, G. *Electronic Materials: The Oligomeric Approach*; Wiley-VCH: Weinheim, 1998.
- (10) Reviews: (a) Bendikov, M.; Wudl, F.; Perepichka, D. F. *Chem. Rev.* **2004**, *104*, 4891. (b) Anthony, J. E. *Chem. Rev.* **2006**, *166*, 5028.
- (11) Selected examples: Ito, S.; Wehmeier, M.; Brand, J. D.; Kübel, C.; Epsch, R.; Rabe, J. P.; Müllen, K. *Chem.—Eur. J.* **2000**, *6*, 4327. Fechtenkötter, A.; Tchebotareva, N.; Watson, M. D.; Müllen, K. *Tetrahedron* **2001**, *57*, 3769. Payne, M. M.; Parkin, S. R.; Anthony, J. E. *J. Am. Chem. Soc.* **2005**, *127*, 8028. Kuninobu, Y.; Seiki, T.; Kanamaru, S.; Nishina, Y.; Takai, K. *Org. Lett.* **2010**, *12*, 5287–5289.
- (12) Cai, J.; Ruffieux, P.; Jaafar, R.; Bieri, M.; Braun, T.; Blankenburg, S.; Mouth, M.; Seitsonen, A. P.; Saleh, M.; Feng, X.; Müllen, K.; Fasel, R. *Nature* **2010**, *466*, 470.
- (13) Template-initiated growth strategy: (a) Fort, E. H.; Donovan, P. M.; Scott, L. T. *J. Am. Chem. Soc.* **2009**, *131*, 16006. (b) Fort, E. H.; Scott, L. T. *Angew. Chem., Int. Ed.* **2010**, *49*, 6626. (c) Fort, E. H.; Scott, L. T. *J. Mater. Chem.* **2011**, *21*, 1373.
- (14) (a) Neenan, T. X.; Whitesides, G. M. *J. Org. Chem.* **1988**, *53*, 2489. (b) Haley, M. M.; Tykwinski, R. R., Eds. *Carbon-Rich Compounds: From Molecules to Materials*; Wiley-VCH: New York, 2006. (c) Diederich, F.; Stang, P. J.; Tykwinski, R. R., Eds. *Acetylene Chemistry: Chemistry, Biology and Material Science*; Wiley-VCH: Weinheim, 2005. (d) Bunz, U. H. F. *Angew. Chem., Int. Ed. Engl.* **1994**, *33*, 1073. (e) Marsden, J. A.; Haley, M. M. *J. Org. Chem.* **2005**, *70*, 10213. (f) Tour, J. M. *Chem. Rev.* **1996**, *96*, 537. (g) Diederich, F.; Rubin, Y. *Angew. Chem., Int. Ed. Engl.* **1992**, *31*, 1101. (h) Gholami, M.; Tykwinski, R. R. *Chem. Rev.* **2006**, *106*, 4997. (i) Shin, Y.; Fryxell, G. E.; Johnson, C. A., II; Haley, M. M. *Chem. Mater.* **2008**, *20*, 981. (j) Johnson, C. A., II; Lu, Y.; Haley, M. M. *Org. Lett.* **2007**, *9*, 3725.
- (15) (a) Giese, B. *Radicals in Organic Synthesis: Formation of Carbon-Carbon Bonds*; Pergamon: Oxford, U.K., 1986. (b) Curran, D. P. *Synthesis* **1988**, 417, 489. (c) Jasperse, C. P.; Curran, D. P.; Fevig, T. L. *Chem. Rev.* **1991**, *91*, 1237. (d) Hildebrandt, D.; Dyker, G. J. *Org. Chem.* **2006**, *71*, 6728. (e) Wang, K. K. *Chem. Rev.* **1996**, *96*, 207. (f) Snider, B. B. *Chem. Rev.* **1996**, *96*, 339. (g) Gansauer, A.; Bluhm, H. *Chem. Rev.* **2000**, *100*, 2771. (h) Renaud, P.; Sibi, M. P., Eds. *Radicals in Organic Synthesis*; Wiley-VCH: Weinheim, Germany, 2001. (i) Sibi, M. P.; Manyem, S.; Zimmerman, J. *Chem. Rev.* **2003**, *103*, 3263.
- (16) Alabugin, I. V.; Gilmore, K.; Patil, S.; Manoharan, M.; Kovalenko, S. V.; Clark, R. J.; Ghiviriga, I. *J. Am. Chem. Soc.* **2008**, *130*, 11535.
- (17) For general discussion of alkyne cyclizations, see: (a) Gilmore, K.; Alabugin, I. V. *Chem. Rev.* **2011**, *111*, 6513. (b) Alabugin, I.; Gilmore, K.; Manoharan, M. *J. Am. Chem. Soc.* **2011**, *133*, 12608. (c) For a discussion of 5-exo/6-endo competition in conjugated systems, see: Alabugin, I. V.; Manoharan, M. *J. Am. Chem. Soc.* **2005**, *127*, 12583.
- (18) Intramolecular activation through the Bergman cyclization also provides complicated mixtures: (a) Grubbs, R.; Kratz, D. *Chem. Ber* **1993**, *126*, 149. (b) Gleiter, R.; Kratz, D. *Angew. Chem., Int. Ed. Engl.* **1993**, *32*, 842.
- (19) Alabugin, I. V.; Manoharan, M. *J. Am. Chem. Soc.* **2005**, *127*, 9534. Alabugin, I. V.; Timokhin, V. I.; Abrams, J. N.; Manoharan, M.; Ghiviriga, I.; Abrams, R. *J. Am. Chem. Soc.* **2008**, *130*, 10984.
- (20) Spectra of fulvene products were analogous to the literature data: Kovalenko, S. V.; Peabody, S.; Manoharan, M.; Clark, R. J.; Alabugin, I. V. *Org. Lett.* **2004**, *6*, 2457. Peabody, S.; Breiner, B.; Kovalenko, S. V.; Patil, S.; Alabugin, I. V. *Org. Biomol. Chem.* **2005**, *3*, 218. For the formation of fulvenes via radical 5-exo-dig cyclization of alkynes, see also: König, B.; Pitsch, W.; Klein, M.; Vasold, R.; Prall, M.; Schreiner, P. R. *J. Org. Chem.* **2001**, *66*, 1742. Lewis, K. D.; Rowe, M. P.; Matzger, A. J. *Tetrahedron* **2004**, *60*, 7191.
- (21) Beckwith, A. L. J.; Easton, C. J.; Serelis, A. K. *J. Chem. Soc. Chem. Commun.* **1980**, 482.
- (22) Prakash, C.; Mohanakrishnan, A. K. *Eur. J. Org. Chem.* **2008**, 1535.
- (23) The cascade product is formed as a ~1:1.1 mixture of two diastereomers. We have tentatively assigned the major product as the more stable trans-isomer.
- (24) Alabugin, I. V.; Manoharan, M.; Breiner, B.; Lewis, F. J. *J. Am. Chem. Soc.* **2003**, *125*, 9329.
- (25) Goldfinger, M. B.; Crawford, K. B.; Swager, T. M. *J. Am. Chem. Soc.* **1997**, *119*, 4578 and ref 8a.
- (26) (a) Shifrina, Z. B.; Averina, M. S.; Rusanov, A. L.; Wagner, M.; Müllen, K. *Macromolecules* **2000**, *33*, 3525. Feng, X.; Pisula, W.; Müllen, K. *Pure Appl. Chem.* **2009**, *81*, 2203. (b) Another conceptually related example is provided by the elegant work of L. Scott, who used sequential Diels-Alder reactions of alkynes to grow walls of carbon nanotubes. Scott, L. T.; Jackson, E. A.; Zhang, Q.; Steinberg, B. D.; Bancu, M.; Li, B. *J. Am. Chem. Soc.* **2012**, *134*, 107 See also ref 13a. and 13b..